

MEASURING STELLAR RADIAL VELOCITIES WITH A DISPERSED FIXED-DELAY INTERFEROMETER

SUVRATH MAHADEVAN¹, JULIAN VAN EYKEN, JIAN GE, CURTIS DEWITT, SCOTT W. FLEMING,
ROGER COHEN, JUSTIN CREPP & ANDREW VANDEN HEUVELAstronomy Department, University of Florida, 211 Bryant Space Science Center P.O. Box 112055
Gainesville, FL 32611-2055
suvrath@astro.ufl.edu*Draft version August 31, 2021*

ABSTRACT

We demonstrate the ability to measure precise stellar barycentric radial velocities with the dispersed fixed-delay interferometer technique using the Exoplanet Tracker (ET), an instrument primarily designed for precision differential Doppler velocity measurements using this technique. Our barycentric radial velocities, derived from observations taken at the KPNO 2.1 meter telescope, differ from those of Nidever et al. by 0.047 km s^{-1} (rms) when simultaneous iodine calibration is used, and by 0.120 km s^{-1} (rms) without simultaneous iodine calibration. Our results effectively show that a Michelson interferometer coupled to a spectrograph allows precise measurements of barycentric radial velocities even at a modest spectral resolution of $R \sim 5100$. A multi-object version of the ET instrument capable of observing ~ 500 stars per night is being used at the Sloan 2.5 m telescope at Apache Point Observatory for the Multi-object APO Radial Velocity Exoplanet Large-area Survey (MARVELS), a wide-field radial velocity survey for extrasolar planets around TYCHO-2 stars in the magnitude range $7.6 < V < 12$. In addition to precise differential velocities, this survey will also yield precise barycentric radial velocities for many thousands of stars using the data analysis techniques reported here. Such a large kinematic survey at high velocity precision will be useful in identifying the signature of accretion events in the Milky Way and understanding local stellar kinematics in addition to discovering exoplanets, brown dwarfs and spectroscopic binaries.

Subject headings: techniques: radial velocities — techniques: spectroscopic — instrumentation: interferometers — instrumentation: spectrographs — stars: kinematics — methods: data analysis

1. INTRODUCTION

The discovery of various tidal streams in our galaxy (Ibata et al. 1994; Yanny et al. 2006; Belokurov et al. 2006) challenges the monolithic collapse formation model (Eggen 1962), but the streams discovered so far form only a small fraction of the mass of the galaxy. Large kinematic surveys are necessary to determine if such merger and accretion events are more common. Radial velocity surveys using multi-object spectrographs, like RAVE (Steinmetz et al. 2006), are already producing barycentric radial velocities for many thousands of stars at a precision of $2 - 3 \text{ km s}^{-1}$, enabling studies of galactic dynamics (e.g. Veltz et al. 2008). In the northern hemisphere the magnitude limited Geneva-Copenhagen Survey (Nordstrom et al. 2004) has provided radial velocities for over 14000 bright nearby F and G dwarfs ($V < 8.6$) at a precision of $100 - 300 \text{ m s}^{-1}$. Coupled with gravity and chemical composition derived from the observed spectra, such datasets of precise barycentric radial velocities are very valuable in identifying past accretion events and substructure in the galactic disk (Helmi et al. 2006), finding members of moving groups (Jones 1970) and determining cluster membership.

The ability to determine precise differential radial velocities has also improved dramatically in the last few years, and planet search surveys are currently at a precision of $1 - 3 \text{ m s}^{-1}$ (Rupprecht et al. 2004; Butler et al. 1996). Such planet search surveys, however, use an arbitrary zero

point for the stellar velocities since only differential velocities are measured. The true radial velocity of the center-of-mass of a star is a difficult quantity to measure accurately using spectroscopy since it involves additional modelling (or assumptions) of effects like convective blue shift and gravitational redshift (Lindgren & Dravins 2003). A quantity that is easier to obtain, in terms of observables and known physical constants, is the apparent Doppler shift of the lines in the stellar spectra, as measured in the solar system barycenter, with the Sun setting the velocity zero point. This Doppler shift can be converted into a velocity that we define as the barycentric radial velocity of the star. Very precise barycentric radial velocities have been measured using high resolution echelle spectrographs by Udry et al. 1999 (UD99 hereafter) for a number of stable F, G, K dwarfs, as well as by Nidever et al. 2002 (ND02 hereafter) for a larger sample.

In this paper we demonstrate the ability of a dispersed fixed-delay interferometer (DFDI) to measure precise barycentric radial velocities. The Exoplanet Tracker (ET) is a prototype of this class of instruments, which use a Michelson interferometer followed by a medium resolution spectrograph working in the first grating order. Fixed delay interferometers have long been used by solar astrophysicists to measure solar oscillations (Gorskii & Lebedev 1977; Kozhevnikov 1983; Harvey et al. 1995). In 1997 D. J. Erskine proposed adding a spectrograph as a post disperser for increasing the measurement precision

¹ Visiting Astronomer, Kitt Peak National Observatory, National Optical Astronomy Observatory. KPNO is operated by AURA, Inc. under contract to the National Science Foundation.

of differential radial velocities (Erskine & Ge 2000; Ge, Erskine & Rushford 2000). When using this technique sinusoidal interference fringes are formed in the slit direction at the position of the stellar absorption lines. A shift in the dispersion direction of the underlying spectra due to a Doppler shift manifests itself as the phase shift of the sinusoidal fringes in the slit direction (Ge 2002).

Precise radial velocities can be measured with DFDI even at low wavelength dispersions since information is also being encoded as sinusoidal fringes in the slit direction. This results in each stellar spectrum taking up only a small fraction of the available number of pixels on the CCD detector used to record the spectrum. This feature of the DFDI technique is a great advantage since it has the potential to enable a multi-object instrument (similar to ET) to simultaneously obtain precise radial velocities for a large number of stars (Ge 2002; Ge et al. 2002) without the need for an expensive cross-dispersed high spectral resolution instrument. One such instrument, the W. M. Keck Exoplanet Tracker, is being used at the Sloan 2.5 m telescope for the magnitude limited Multi-object APO Radial Velocity Exoplanet Large-area Survey (MARVELS), a survey for extrasolar planets around TYCHO-2 stars in the magnitude range $7.6 < V < 12$ that is being conducted as part of SDSS III (Weinberg et al. 2007). This instrument can observe 59 stars simultaneously, and approximately 500 stars per night. Designed primarily as a wide-field precision radial velocity survey to discover short and intermediate period planets, MARVELS will also provide a dataset of precise barycentric radial velocities for thousands of late F, G, and K TYCHO-2 stars.

2. OBSERVATIONS

The observations presented in this article were conducted with the single object ET instrument at the Kitt Peak 2.1 meter telescope in January 2006 as part of an ongoing planet search program. The ET instrument is linked to the telescope by a 200 μm optical fiber, which is fed by the f/8 beam of the 2.1 meter telescope. The instrument itself is housed in an isolated room in the basement and consists of a Michelson interferometer in series with a medium resolution spectrograph operating in the wavelength range 5000 – 5640 \AA , and with a spectral resolution of $R \sim 5100$. An iodine cell can be inserted into the optical path and serves to calibrate out instrument drifts. This instrument has successfully demonstrated its short-term stability by confirming known planets (e.g. van Eyken et al. 2004) and discovering a short period planet around the star HD102195 (Ge et al. 2006).

The observing procedure for the ET planet search program is similar to other precision radial velocity programs that use an iodine cell to calibrate out the instrument drifts (e.g. Butler et al. 1996). For each star in the program a single exposure is acquired without the iodine cell inserted in the beam path. An exposure of the iodine cell, illuminated by a tungsten lamp, is also acquired immediately before or after this stellar exposure. These exposures are referred to as the star and iodine template respectively. The iodine template is acquired at high signal to noise (S/N), typically $S/N = 150\text{-}200$ per pixel. The signal-to-noise on the star template depends on the brightness of the star and the exposure time and is generally in the range

of $S/N = 50\text{-}200$ per pixel. All subsequent exposures are taken with the iodine cell inserted in the path of the stellar beam. It is from these exposures that precision radial velocities are obtained since the velocity drift of the iodine component tracks the instrument drift, allowing it be calibrated out. Exposure times are similar to those used on the stellar template, typically yielding a $S/N \sim 1/\sqrt{2}$ of that obtained on the stellar template (since the iodine cell absorbs almost 50% of the light).

Stable stars and known planet-bearing stars are routinely observed for calibration as part of the ET planet search program. During the observing run we were able to obtain regular observations of the RV stable stars η Cas (small linear trend in velocity), τ Ceti, and 36 Uma as well as the known planet bearing stars 51 Peg (Mayor & Queloz 1995), 55 Cnc (McArthur et al. 2004), and HD4967 (Butler et al. 2003). For six stars, chosen because they had rms velocity scatter less than 100 m s^{-1} reported in ND02 (HD3674, HD3861, HD12414, HD105405, HD130087, HD134044), we also acquired stellar templates and iodine templates immediately before or after the respective stellar templates, although no star-with-iodine data points were obtained for these six stars. Typical exposure times varied from 3 minutes for the brightest star (η Cas, $V = 3.45$) to 10 minutes for the faintest (HD130087, $V = 7.52$), leading to a photon noise limited radial velocity error of $3 - 10 \text{ m s}^{-1}$ for most observations.

The advantage of an isolated, fiber-fed instrument is the potential for high stability. The total instrument velocity drift during the observing run (as tracked by the iodine templates) can be seen in Figure 1. The instrument velocity drift is only 2.5 km s^{-1} over the entire 12 day observing run and less than 0.5 km s^{-1} over the first night. This short term stability is essential for the data analysis technique described in Section 3.1.

3. DATA ANALYSIS PROCEDURE

The standard ET data analysis pipeline was designed to extract differential radial velocity for the planet search program. It does not give the barycentric radial velocity of the star since the zero point itself is arbitrary. The pipeline processing steps are described in more detail in van Eyken et al. 2004, and Ge et al. 2006. Here we discuss the various processing steps briefly, but we concentrate on the modifications that allow barycentric radial velocities to be measured.

The data produced by ET were processed using standard IRAF procedures, as well as software written in Research System Inc.’s IDL software. The images were corrected for biases, dark current, and scattered light and then trimmed, illumination corrected, and low-pass filtered. The visibilities (V) and the phases (θ) of the fringes were determined for each channel by fitting a sine wave to each column of pixels in the slit direction, with the fringe visibility, V , being defined as

$$V = (I_{max} - I_{min}) / (I_{max} + I_{min}) \quad (1)$$

where I_{max} and I_{min} are the maximum and minimum values of the fitted sine wave. A wavelength calibration was applied using the observed Thorium-Argon spectra, and the visibility and phase data were dispersion corrected and re-binned to a log-lambda wavelength scale. To determine differential velocity shifts in the star+iodine data

(starlight passing through the iodine cell) the data can, to a good approximation, be considered as a summation of the complex visibilities ($\mathbf{V} = Ve^{i\theta}$) of the relevant star ($V_S e^{i\theta_{S_0}}$) and iodine ($V_I e^{i\theta_{I_0}}$) templates (van Eyken et al. 2004; Erskine 2003). For small velocity shifts the complex visibility of the data can be written as

$$V_D e^{i\theta_D} = V_S e^{i\theta_{S_0}} e^{i\theta_S - i\theta_{S_0}} + V_I e^{i\theta_{I_0}} e^{i\theta_I - i\theta_{I_0}} \quad (2)$$

where V_D , V_S , and V_I are the fringe visibilities for a given wavelength in the star+iodine data, star template and iodine template respectively, and θ_D , θ_{S_0} , and θ_{I_0} the corresponding measured phases. In the presence of real velocity shift of the star and instrument drifts the complex visibilities of the star and iodine template best match the data with a phase shift of $\theta_S - \theta_{S_0}$ and $\theta_I - \theta_{I_0}$ respectively. The iodine is a stable reference and the iodine phase shift tracks the instrument drift. The difference between star and iodine shifts is the real phase shift of the star, $\Delta\phi$, corrected for any instrumental drifts

$$\Delta\phi = (\theta_S - \theta_{S_0}) - (\theta_I - \theta_{I_0}) \quad (3)$$

This phase shift can be converted to a velocity shift (Δv) by a known phase-to-velocity scaling factor that is a function of the optical delay in the Michelson interferometer (d), the wavelength (λ) and the speed of light (c). These parameters are connected by the relation

$$\Delta v = \frac{c\lambda}{2\pi d} \Delta\phi \quad (4)$$

In reality the phase shifts of the star and iodine templates are not the only free parameters needed to fit the observed data. The Doppler velocity shift of the star induces a wavelength shift of the entire spectrum and instrument instabilities can lead to pixel shifts relative to the templates. Finding the correct phase shifts requires that these wavelength shifts (or pixels shifts) for the star and iodine templates also be fit simultaneously with the phase shift parameters.

To determine barycentric radial velocities we used the stellar template of a star with known barycentric radial velocity (η Cas) in place of the target star template in Equation 2. The visibility of the reference star was allowed to scale to partially compensate for the template mismatch. The stellar visibility depends on the line depth and width (Ge 2002), and allowing it to scale is in effect similar to attempting to match the line depths and widths of the stellar template with that of the observed star. Similar spectral-morphing techniques have been used (Johnson et al. 2006) with high-resolution echelle data from the N2K survey to achieve short term differential velocity precision of $\sim 5 \text{ m s}^{-1}$ without the need for a stellar template.

3.1. Radial Velocity using Templates Alone

The stability of the ET instrument (Figure 1) makes it possible to attempt to extract the radial velocity without using simultaneous calibration with the iodine cell. When the cell is not inserted into the optical path, the resulting observations of the star can explicitly be modelled as the template spectrum with a phase shift added (the template spectrum may also be the stellar template of a reference star)

$$V_D e^{i\theta_D} = V_S e^{i\theta_{S_0}} e^{i\theta_S - i\theta_{S_0}} \quad (5)$$

In such a case the phase shift, $\theta_S - \theta_{S_0}$, is a combination of the velocity shift of the star compared to the template

and the instrument drift. When using this technique the ET observing procedure requires all star-only exposure to have an iodine template taken immediately before or after the exposure. If the instrument is stable enough, these iodine exposures can be used to determine and calibrate out the instrument drifts for the star exposures. This is only possible when the instrumental velocity drifts are small in the time interval between the exposure mid-points of the star and iodine templates.

Using the entire spectral range of $\sim 640 \text{ \AA}$ a cross-correlation was performed in log-lambda space using the visibilities (V) of the reference star and the target star. The purpose of this cross-correlation was to yield an approximate velocity shift, accurate to $\sim 1-2 \text{ km s}^{-1}$, which is useful as a first guess starting point to calculate a more precise velocity shift using both the visibility and phase information.

The velocity extraction algorithm that is part of the ET pipeline was used to minimize the residuals between the complex visibilities (\mathbf{V}) of the reference star and the target star by varying the phase shift applied to the reference template complex visibility. The visibility of the reference star was also allowed to scale in the fitting procedure in an attempt to minimize the template mismatch, as described in the previous section. This technique yields a phase shift $\theta_S - \theta_{S_0}$ that is a measure of the difference in velocity between the stellar template used and the target star.

To account for instrument drifts between the reference star template and the target star, a similar analysis procedure was followed for the iodine templates (taken very close in time to the reference and target star exposure) with the only difference being that the iodine visibility was not allowed to scale (since there is no template mismatch between iodine cell spectra taken at different times). The phase drift between the two iodine templates is a direct measure of the instrument drift. Subtracting off the iodine phase shift corrects for the instrument drift, giving the real phase shift of the target star with respect to the reference star.

3.2. Radial Velocity from Star+Iodine Data

In the normal data acquisition mode the stellar beam passes through the iodine cell. Cross-correlation with the visibilities from a reference stellar template alone is not appropriate since the iodine spectrum is also present in the data. Using Equation 2 we can write

$$V_D^2 = V_S^2 + V_I^2 + 2V_S V_I \cos(\theta_S - \theta_I) \quad (6)$$

The term $2V_S V_I \cos(\theta_S - \theta_I)$ has an expectation value close to zero over the 640 \AA wavelength band since the cosine term fluctuates randomly. We ignored this term and approximated the visibilities as adding in quadrature ($V_D^2 \approx V_S^2 + V_I^2$). This allowed us to use the TODCOR algorithm (Zucker & Mazeh 1994) on the ensemble of measured visibilities to determine the approximate velocity shifts of the star and iodine templates that are a best fit to the data. The TODCOR algorithm is a two dimensional cross-correlation technique generally used to determine the individual radial velocities of both components of a spectroscopic binary, and can be applied in this case since the two components are approximately additive. Since a reference stellar template for a different star (η Cas) was being used, a visibility scaling was derived using mean visibilities

and Equation 6, and used to scale the stellar visibilities for TODCOR. The scaling factor in visibilities accounts partially for the mismatch in stellar templates. The approximate radial velocity values derived using TODCOR were useful in determining the correct phase shift when the shift was more than $\pm 2\pi$. These radial velocities were used as a first guess to determine the correct wavelength-shift and phase-shift of the stellar and iodine templates that minimized the residuals in the complex visibility between the data and the best fit solution. Subtracting off the iodine phase shift gives the phase shift of the target star with respect to the reference star, corrected for instrument drift.

4. RADIAL VELOCITY RESULTS

The differential radial velocity precision of one of the reference stars, η Cas, is shown in Figure 2. These velocities were extracted using the techniques described in Section 3, but with an arbitrary zero-point. In the case of η Cas the velocity results are identical to those obtained using the standard pipeline since this object is the reference star. The velocity rms of $\sim 6.4 \text{ m s}^{-1}$ is due to a combination of photon noise errors in the data and the templates and systematic errors in the velocity extraction. We used this star as the stellar reference template to determine barycentric radial velocities. Velocities for all the stars are calculated relative to η Cas, requiring prior knowledge the barycentric radial velocity of η Cas itself to apply the correct velocity offset. We used the η Cas mean barycentric radial velocity from ND02 (8.314 km s^{-1}). η Cas is known to be a long-period binary, whose velocity is well fit with a linear trend. We transformed the ND02 velocity to our epoch of observation by applying a correction term for its known $9.3 \text{ m s}^{-1} \text{ year}^{-1}$ linear velocity drift (Cummings et al. 1999). Any error in the determination of this velocity is a error in the zero-point itself, and will affect all target stars in a similar way. The phase difference of each star from the η Cas stellar template was converted to velocity using the phase-to-velocity scaling parameter ($c\lambda/2\pi d$). This radial velocity was then corrected to the solar system barycenter by removing the barycentric velocity contribution of the telescope, calculated with software written in IDL that use the JPL ephemeris. These algorithms are accurate to better than $\sim 2 \text{ m s}^{-1}$. The corrected barycentric radial velocity of η Cas was added to obtain the barycentric radial velocity of the star.

4.1. Radial Velocity Results from Templates Alone

Barycentric radial velocities were derived using the procedure outlined in Section 3.1. A comparison of these velocities with those published by ND02 is shown in Figure 3. No attempt has been made to correct the velocities for the known planetary companions to 51 Peg, 55Cnc and HD49674, which may cause additional velocity scatter. Our velocities agree well with those of ND02 and show a scatter of 120 m s^{-1} , with a mean offset of $-79 \pm 25 \text{ m s}^{-1}$. The agreement of our results with those of ND02 confirms the validity of using the iodine templates to remove the instrument drift when such drifts are small (Figure 1). For example, the typical instrument drift over the first night is approximately 10 m s^{-1} over a 15-minute exposure. Such exposure times with the ET instrument allow the radial velocity of an 11th magnitude ($V=11$) star to

be determined at this level of precision (100 m s^{-1}).

4.2. Radial Velocity Results from Star+Iodine Data

When the required precision is high, it is perhaps more appropriate to use the star+iodine data since the iodine tracks the instrument drift exactly. For all the reference and planet bearing stars, the barycentric radial velocities obtained for all data points (using η Cas as template), derived using the procedure outlined in Section 3.2, were averaged together to give a mean barycentric radial velocity for each star. These radial velocities are shown in Figure 4 and display a rms scatter of 47 m s^{-1} with a mean offset of $-3 \pm 19 \text{ m s}^{-1}$ in comparison with ND02.

4.3. Systematic Errors and Velocity Zero Point

Tests with twilight solar spectra as the reference stellar template show similar levels of rms scatter to those using η Cas, but the twilight observation of the solar spectrum (instead of day sky) introduced an offset in the velocities when the solar spectrum was used as the template. Our results depend on the velocity of η Cas derived by ND02 who use the National Solar Observatory (NSO) solar spectrum (Kurucz et al. 1984) as the stellar template with a 522 m s^{-1} offset to make the radial velocity of the Sun zero. Due to the use of the same zero point our estimated velocities will exhibit similar systematic errors with spectral type as ND02, in addition to any template mismatch effects introduced due to our use of η Cas (G0V) instead of the Sun (G2V).

A number of systematic errors can occur in velocity determination using this technique. Fast rotators ($v \sin i > 12 \text{ km s}^{-1}$) have very low fringe visibilities at our chosen interferometer optical delay (7 mm), leading to a significantly reduced velocity precision for such stars. Incorrect calibration of the interferometer delay can lead to errors in the phase-to-velocity scaling, causing errors in the calculated radial velocity. Our reference (η Cas) has a small linear drift in velocity that we have accounted for using the mean epoch of observation in ND02. An error in this determined barycentric radial velocity of η Cas will appear as a shift in the mean offsets reported here. The stars with known planets have additional velocity variability due to their companions. This variability is reduced when using star+iodine data (Section 4.2) and averaging all the observed velocities, especially for the short period planets 51 Peg and HD49674 that have orbital periods less than our 12 day observing run. The multi-planet 55 Cnc system (McArthur et al. 2004), though, has long period planets which affect the calculated radial velocity. For each star in their sample ND02 report only the mean of the observed barycentric radial velocities, and to ensure a consistent comparison we have made no attempt here to correct our data for these known planetary companions. In general, velocity corrections for known companions is easy to implement if the orbital parameters are known, but we have not done so for consistency with ND02.

5. DISCUSSION

We have demonstrated the ability to measure barycentric radial velocities at a high level of precision (rms = $50 - 120 \text{ m s}^{-1}$) using a dispersed fixed delay interferometer instrument. Our results also show that the radial

velocities derived using a very different technique and an instrument at substantially lower resolution are not very different in precision from those derived using high resolution spectroscopy and cross-correlation with stellar (ND02; UD99) or Fe I line templates (Gullberg & Lindegren 2002). Simultaneous calibration with the iodine cell yields more precise velocities, but the data analysis using only the templates (Section 3.1, 4.1) may be more appropriate for faint stars where the low signal to noise may introduce significant errors when extracting velocities from the star+iodine data. We have corrected the observed radial velocities to the barycenter of the solar system. Using the corrected η Cas radial velocity from ND02 to set the velocity scale for our radial velocities then automatically corrects all velocities for the gravitational redshift and convective blueshift of the Sun (used by ND02 as the zero point). By adopting the radial velocity of η Cas from ND02 we have automatically adopted ND02 as our velocity reference for the absolute calibration of a zero-point and performed a secondary measurement to determine the velocities of all our other target stars. No attempt is made to further correct the stellar radial velocities for spectral type and luminosity class dependent effects. This results in our derived velocities having typical accuracies of $0.2 - 0.3 \text{ km s}^{-1}$ (derived from ND02, our velocity reference) for late F, G and K dwarfs, and precisions of $\sim 50 - 100 \text{ m s}^{-1}$ when comparing stars of similar spectral types. With the ET instrument scheduled to be a facility instrument at the KPNO 2.1m, this velocity measurement capability will be available to the wider astronomical community. These techniques will

also be applied to data from the MARVELS survey that will observe $\sim 10,000$ stars as part of SDSS III, leading to precise barycentric radial velocities being measured for the majority of the stars in the sample.

Future work with these instruments will focus on using the day sky spectra of the Sun as a stellar template to determine the velocity zero point, allowing independent comparison with the radial velocities of ND02 and UD99 without having to adopt either of these works as the velocity reference, and a better understanding of any zero point differences that may arise due to the much lower spectral resolution (Dravins & Norlund 1990) of ET compared to high resolution echelle spectrographs.

We are grateful to Richard Green, Skip Andree, Daryl Wilmarth and the KPNO staff for their generous support. We would also like to thank the anonymous referee for a careful reading of the manuscript and for very constructive suggestions. This work is supported by National Science Foundation grant AST 02-4309, JPL, the Pennsylvania State University, and the University of Florida. J. v. E. and S.M. acknowledge travel support from KPNO and the Michelson Fellowship. This research has made use of the SIMBAD and VizieR databases, operated at ADC, Strasbourg, France. This work was performed in part under contract with the Jet Propulsion Laboratory (JPL) funded by NASA through the Michelson Fellowship Program. JPL is managed for NASA by the California Institute of Technology. This work is based on data obtained at the Kitt Peak 2.1m telescope.

REFERENCES

- Belokurov, V., Evans, N. W., Irwin, M. J., Hewett, P. C., & Wilkinson, M. I. 2006, *ApJ*, 637, L29
- Butler, R. P., Marcy, G. W., Williams, E., McCarthy, C., Dosanjh, P., & Vogt, S. S. 1996, *PASP*, 108, 500
- Butler, R. P., Marcy, G. W., Vogt, S. S., Fischer, D. A., Henry, G. W., Laughlin, G., & Wright, J. T. 2003, *ApJ*, 582, 455
- Cumming, A., Marcy, G. W., & Butler, R. P. 1999, *ApJ*, 526, 890
- Dravins, D., & Nordlund, A. 1990, *A&A*, 228, 203
- Erskine, D. J., & Ge, J. 2000, *ASP Conf. Ser.* 195: *Imaging the Universe in Three Dimensions*, 195, 501
- Erskine, D. J. 2003, *PASP*, 115, 255
- Erskine, D. J., Edelstein, J., Harbeck, D., & Lloyd, J. 2005, *Proc. SPIE*, 5905, 249
- Ge, J. 2002, *ApJ*, 571, L165
- Ge, J., Erskine, D. J., & Rushford, M. 2002, *PASP*, 114, 1016
- Ge, J., et al. 2006, *ArXiv Astrophysics e-prints*, arXiv:astro-ph/0605247
- Gorskii, S. M., & Lebedev, V. P. 1977, *Izvestiya Ordena Trudovogo Krasnogo Znameni Krymskoj Astrofizicheskij Observatorii*, 57, 228
- Gullberg, D., & Lindegren, L. 2002, *A&A*, 390, 383
- Harvey, J., & The GONG Instrument Team 1995, *ASP Conf. Ser.* 76: *GONG 1994. Helio- and Astro-Seismology from the Earth and Space*, 76, 432
- Helmi, A., Navarro, J. F., Nordström, B., Holmberg, J., Abadi, M. G., & Steinmetz, M. 2006, *MNRAS*, 365, 130
- Ibata, R. A., Gilmore, G., & Irwin, M. J. 1994, *Nature*, 370, 194
- Johnson, J. A., et al. 2006, *ApJ*, 647, 600
- Jones, B. F. 1970, *AJ*, 75, 56
- Kozhevnikov, I. E. 1983, *Izslidovaniia Geomagnetizmu Aeronomii i Fizike Solntsa*, 64, 42
- Kurucz, R. L., Furenlid, I., Brault, J., & Testerman, L. 1984, *National Solar Observatory Atlas, Sunspot, New Mexico: National Solar Observatory*, 1984,
- Lindegren, L., & Dravins, D. 2003, *A&A*, 401, 1185
- McArthur, B. E., et al. 2004, *ApJ*, 614, L81
- Mahadevan, S., Ge, J., van Eyken, J. C., DeWitt, C., & Shaklan, S. B. 2003, *Proc. SPIE*, 5170, 184
- Marcy, G. W., Butler, R. P., Williams, E., Bildsten, L., Graham, J. R., Ghez, A. M., & Jernigan, J. G. 1997, *ApJ*, 481, 926
- Nidever, D. L., Marcy, G. W., Butler, R. P., Fischer, D. A., & Vogt, S. S. 2002, *ApJS*, 141, 503
- Nordström, B., et al. 2004, *A&A*, 418, 989
- Rupprecht, G., et al. 2004, *Proc. SPIE*, 5492, 148
- Steinmetz, M., et al. 2006, *ArXiv Astrophysics e-prints*, arXiv:astro-ph/0606211
- Udry, S., Mayor, M., & Queloz, D. 1999, *ASP Conf. Ser.* 185: *IAU Colloq. 170: Precise Stellar Radial Velocities*, 185, 367
- van Eyken, J. C., Ge, J., Mahadevan, S., & DeWitt, C. 2004, *ApJ*, 600, L79
- Veltz, L., et al. 2008, *ArXiv e-prints*, 801, arXiv:0801.2120
- Weinberg, D. H., et al. 2007, *American Astronomical Society Meeting Abstracts*, 211, #132.10
- Yanny, B., et al. 2003, *ApJ*, 588, 824
- Zucker, S., & Mazeh, T. 1994, *ApJ*, 420, 806

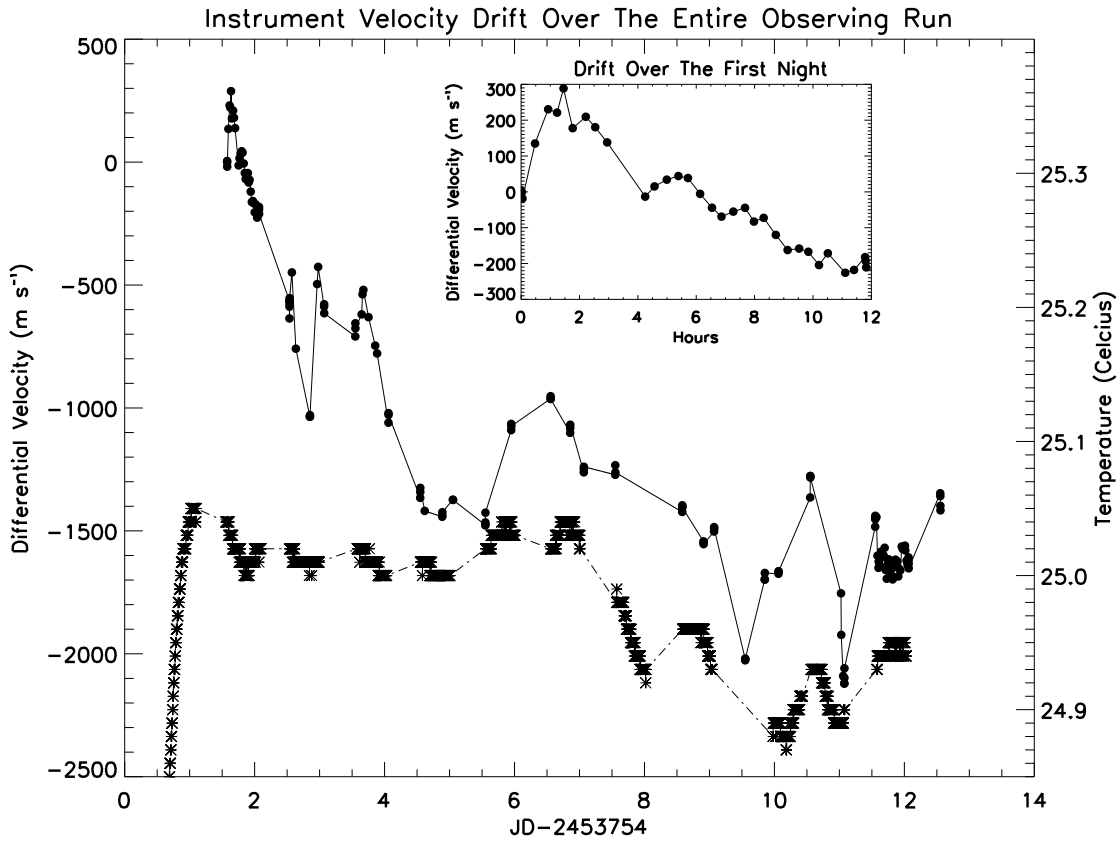


FIG. 1.— Velocity drift of the ET instrument. The solid line is the velocity drift as tracked by the iodine templates (filled circles). The dashed line tracks the temperature drift of the Michelson interferometer (asterisks). A loose correlation between the temperature drifts and the velocity drifts is evident. Instrument stability is essential for obtaining radial velocities if the simultaneous iodine calibration is not used.

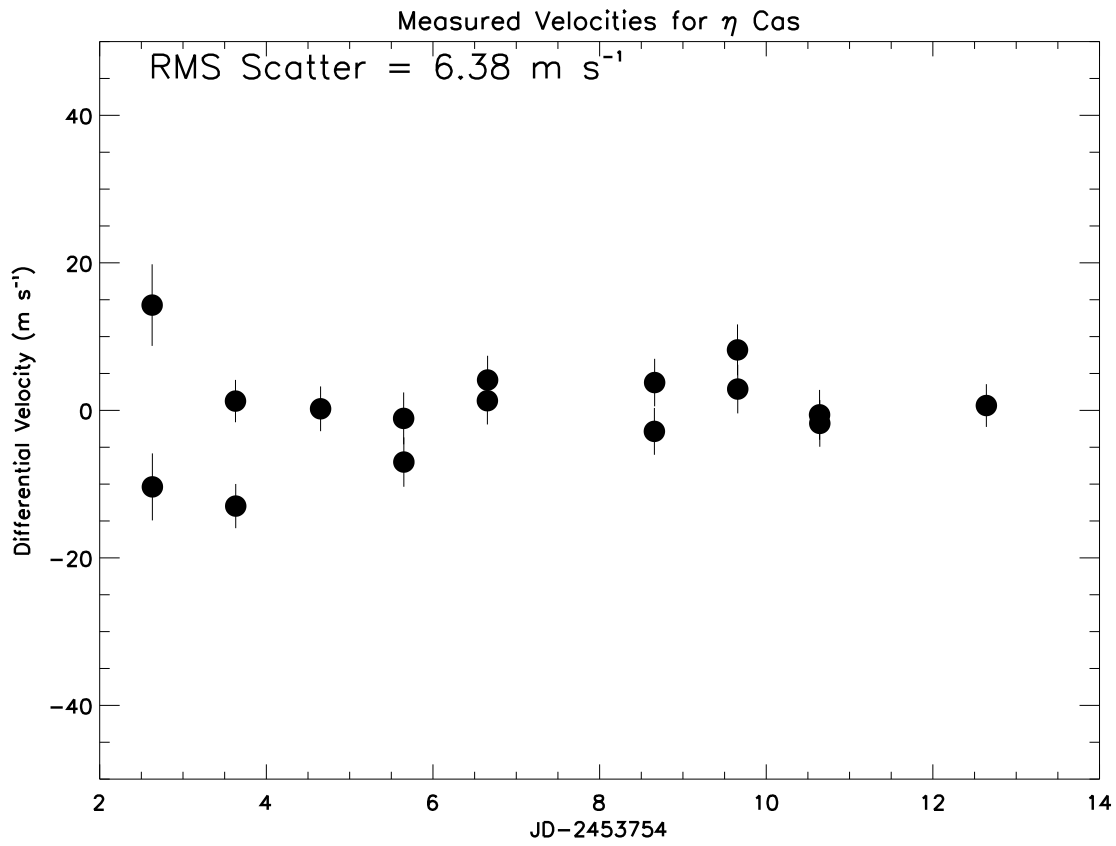


FIG. 2.— Differential radial velocity observations of the star η Cas with ET. The rms velocity scatter of $\sim 6.4 \text{ m s}^{-1}$ is caused by a combination of photon noise errors and systematic errors. This star is used as the stellar template to determine barycentric radial velocities (see Section 4).

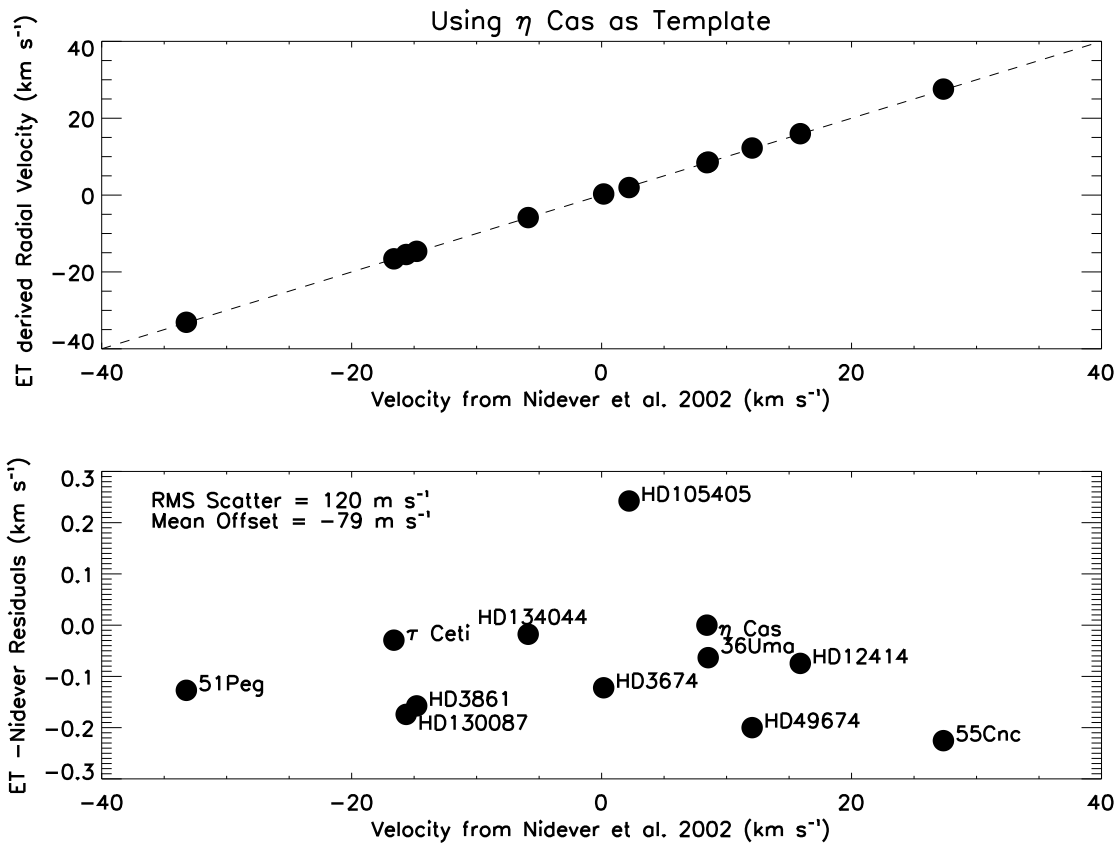


FIG. 3.— Comparison of radial velocities obtained by ET, from stellar and iodine templates alone, with ND02. The comparison of ET velocities with ND02 velocities yields an rms velocity scatter of 120 m s^{-1} .

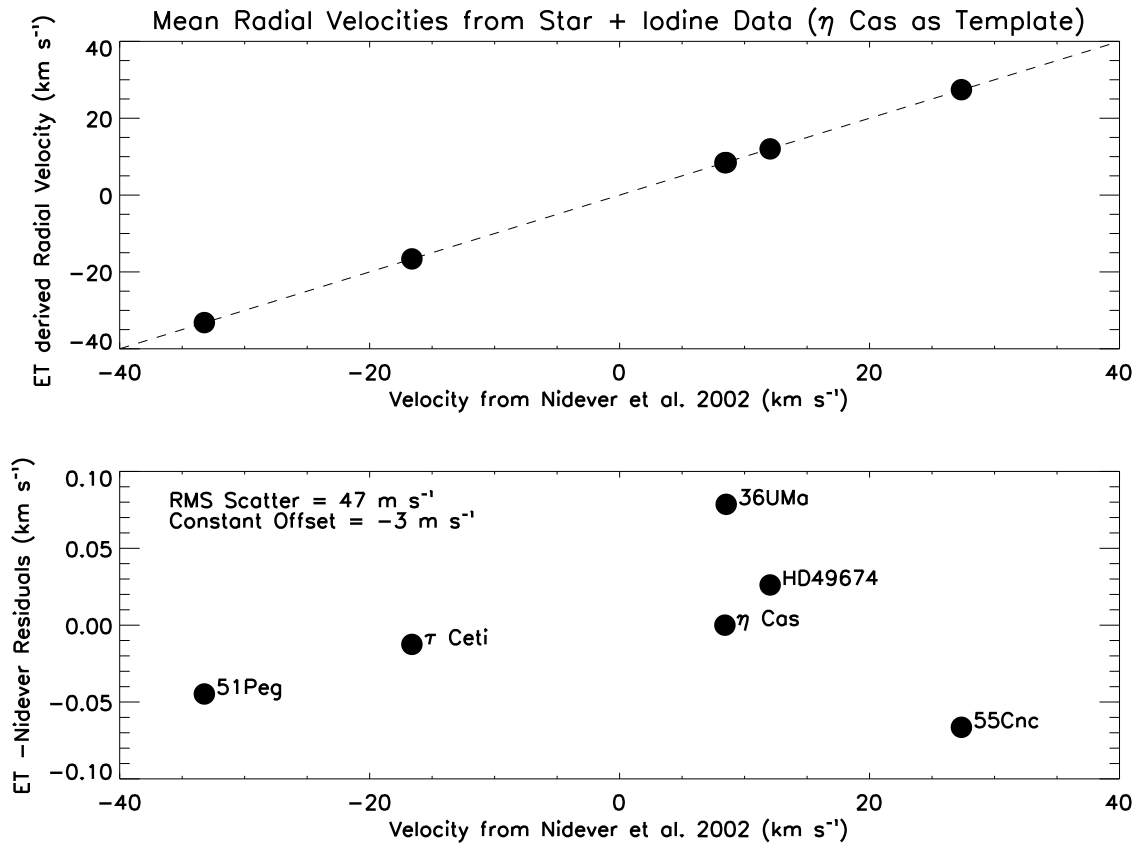


FIG. 4.— Residuals of the average ET radial velocities derived from star+iodine data from the velocities of ND02. Residuals show an rms velocity scatter of 47 m s^{-1} .